Journal of Computational Applied Mechanics 2023, 54 (2): 219-235

DOI: 10.22059/jcamech.2023.356976.817

RESEARCH PAPER

Fourier-homotopy perturbation method for heat and mass transfer with 2D unsteady squeezing viscous flow problem

Yasir Ahmed Abdul-Ameer *, Abdul-Sattar Jaber Ali Al-Saif

Department of Mathematics, college of Education for Pure Science, Basrah University, Basrah, Iraq.

Abstract

In this article, the homotopy perturbation method (HPM) and Fourier transform (FT) were combined to construct a hybrid method that can be represented by the symbol (FT-HPM), the new technique succeeded to find an approximate solution for the model of heat and mass transfer in the unsteady squeezing flow between parallel plates analytically. The similarity transformation methodology was relied upon to convert a system of partial differential equations into a system of ordinary differential equations. The influence of physical parameters (squeeze number, Prandtl number, Schmidt number and the Eckert number) on velocity, temperature and concentration with different values is discussed. In addition, the physical quantities represented by the Nusselt number, Sherwood number, and the skin friction coefficient were studied, and the new numerical results of these quantities were compared with the results of previously published works. Finally, the convergence of the new method was studied theoretically by formulating the basic convergence theorem. In addition, this theorem was applied to the results of the solutions obtained using FT-HPM. The tables and graphs of the new analytical solutions showed the possibility and usefulness of using the new algorithm to deal with many non-linear problems, especially natural convection problems.

Keywords: Homotopy perturbation method, Fourier transform, Heat and mass transfer, Unsteady squeezing flow, convergence analysis.

1. Introduction

For decades, scientists and engineers have been interested in studying the theory of viscous flow, especially the flow of Newtonian and non-Newtonian fluids, because of its wide applications in various branches of science and technology. Many of these applications can be described by ordinary or partial nonlinear differential equations. In recent years, many powerful methods have been developed to obtain approximate solutions of nonlinear differential equations. The problem of heat and mass transfer combined with unsteady two-dimensional squeezing viscous flow have received the attention of many authors because there are many scientific and engineering applications for this problem, such as food processing, cooling towers, drying, chemical processing equipment, and surface evaporation. and polymer processing, hydrodynamic machines, etc. The researchers succeeded in presenting many theoretical and experimental studies on the mentioned problem. Let's take an example, Mahmood et al. [1] used the perturbation method, asymptotic method and the local non-similarity method to solve the problem of flow and heat transfer over a permeable sensor surface placed in a squeezing channel. This study illustrated that the solutions of local non-similarity agree with the solutions of perturbation for large and small values of the local transpiration parameter. The 2D unsteady flow with heat and mass transfer of viscous fluid between the infinite parallel plates was solved by Mustafa et al. [2], relying on similarity transformation and the homotopy analysis method (HAM), the study showed that only the tenth-order of approximation leads to convergent solutions. Sheikholeslami [3] applied the Adomian decomposition method (ADM) to simulate the model of unsteady squeezing nanofluid flow and heat transfer. And also, Sheikholeslami et al. [4] used the homotopy perturbation method (HPM) to analyze the problem of two phase

* Corresponding Author: Email: pepg.yasir.ahmed@uobasrah.edu.iq

nanofluid flow and heat transfer between parallel plates which includes the thermophoresis and the effects of Brownian motion. Pourmehran et al. [5] proposed the least square method (LSM), collocation method (CM) and the method of fourth-order Runge-Kutta to study the unsteady flow problem of a nanofluid squeezing between two parallel plates. they found that the results of the LSM are more accurate than the results of the CM when compared with the results of the numerical method. In addition, the Runge-Kutta-Fehlberg method and the shooting technique were applied to solve the heat and mass transfer behaviour of the unsteady flow problem of squeezing nanofluid between two parallel plates in the sight of a uniform magnetic field with slip velocity effect by Singh et al. [6]. HPM was also used by Sobamowoa and Akinshiloa [7] to study and analyze the double diffusive squeezing unsteady flow problem of electrically conducting nanofluid between two parallel disks under slip and temperature jump condition. The differential transform method (DTM) was applied to investigate the heat and mass transfer problem in unsteady two-dimensional MHD squeezing flow of Eyring-Powell fluid between two parallel infinite plates by Balazadeh et al. [8], when comparing the results of DTM and Runge-Kutta-Fehlbrg method, it was found that there is a good agreement between the two methods. Atlas et al. [9] presented an experimental study for the problem of entropy generation on 2D unsteady Casson fluid flow squeezing between two parallel plates using similarity transformation and the shooting method. They applied Cattaneo Christov heat and mass flux instead of using Fourier's and Fick's laws. Al-Saif and Harfash [10] used the perturbation-iteration algorithm (PIA) to study heat and mass transfer in the unsteady squeezing flow between parallel plates. The similarity transformation was used to transform the partial differential equations governing the problem into a system of ordinary differential equations. Moreover, the influence of physical parameters on velocity, temperature and concentration with different values is discussed. In addition, the convergence of the analytical solutions obtained by the proposed method was discussed. The numerical results of the coefficients of skin friction, Nusselt number (*Nu*) and Sherwood number (*Sh*) were also compared with those of previously published works.

Despite the advantages of the previous methods and their ability to find numerical and analytical solutions to non-linear problems, in particular the problems of heat transfer by natural convection, many of these methods are not without some difficulties represented by high arithmetic operations, and some of them require large time and effort to get the required solution, such as HPM, HAM and ADM. Besides what has been mentioned, many integral transformations (Laplace transform (LT), Fourier transform (FT), Yang transform (YT), ...) can be used to solve linear problems, but it is often difficult to use these transformations to find the required solutions for some non-linear problems. What has been presented prompts us to propose a new algorithm through which we seek to address some of the difficulties mentioned in the previous methods used to find a solution to such problems. Relying on the information we obtained from previous studies, it was noted that the combination of approximate analytical methods and integrative transformations may be help to reduce many of the difficulties that researchers face when using each method separately. Therefore, it was proposed to combine the homotopy perturbation method with the Fourier transform to find a hybrid procedure that can be denoted by the symbol (FT-HPM). The most important characteristics of this method is to reduce the computations related to the integrative operations when using the homotopy perturbation method individually. Moreover, the property of convolution theory can be applied in the new method in order to reduce the difficulty of using Fourier transform in solving non-linear differential equations. In this paper, the algorithm of FT-HPM was applied in order to find an analytical approximate solution to the problem of heat and mass transfer with unsteady 2D squeezing viscous flow. the effect of physical parameters on velocity, temperature and concentration with different values was investigated with different values. The numerical results of the coefficients of skin friction, *Nu* and *Sh*, were also compared with those of previously published studies [2, 3, 5, 10-12]. In addition, the convergence of the analytical solutions obtained by the proposed method was proven. The research is organized as the following, in section 2, the basic idea of the HPM is presented. In section 3, the main algorithm is built featuring an expansion of the homotopy perturbation method using Fourier transform. Section 4 contains the governing mathematical equations of the mathematical model. In section 5, the main steps of algorithm (FT-HPM) are applied on the mathematical model. Section 6 contains the results and discussion. In section 7, the convergence analysis of approximate analytical solutions of the proposed method is studied.

2. Basic Idea of Homotopy Perturbation Method

The homotopy perturbation method (HPM) was established by He J. Huan [13, 14]. This method is a powerful and efficient technique for solving differential and integral equations, linear and nonlinear. This method has a great advantage because it provides an approximate solution to a wide variety of nonlinear problems in applied science. In this method the solution is considered as the summation of an infinite series, [15]. To explain the idea of this method, let us consider the following non-linear differential equation:

$$A(u) - q(x) = 0, x \in \Omega, \tag{1a}$$

subject to the boundary conditions

$$B(u, \frac{\partial u}{\partial n}) = 0, x \in \Gamma. \tag{1b}$$

Where, A represent a general differential operator, u is the unknown function, $q(x)$ is a known analytic function, B is a boundary operator, and Γ is the boundary of the domain Ω. The operator A can be generally decomposed into two operators, L and N, where L is a linear operator and N is a nonlinear operator. Moreover, Eq. (1a) can be rewritten as follows:

$$L(u) + N(u) - q(x) = 0. \tag{1c}$$

By using the homotopy perturbation technique, we construct a homotopy $U(x,p)$: $\Omega \times [0,1] \longrightarrow \mathbb{R}$, which satisfies

$$H(U,p) = (1-p)[L(U) - L(u_0)] + p[A(U) - q(x)] = 0, \tag{2a}$$

Or

$$H(U,p) = L(U) - L(u_0) + pL(u_0) + p[N(U) - q(x)] = 0, \tag{2b}$$

where $p \in [0,1]$ is an impeding parameter and u_0 is an initial approximation for the solution of Eq. (1a), which satisfies the boundary conditions. Obviously, from Eq. (2a) or Eq. (2b), we will have

$$\begin{aligned} H(U,0) &= L(U) - L(u_0) = 0, \\ H(U,1) &= A(U) - q(x) = 0. \end{aligned} \tag{3}$$

Therefore, the solution of Eq. (2a) or Eq. (2b) can be expressed as a power series in term of p as follows:

$$U = \sum_{j=0}^{\infty} p^j U_j \tag{4}$$

Setting $p = 1$, then the approximate solution of Eq. (1a) can be given by

$$u = \lim_{p \to 1} U = \sum_{j=0}^{\infty} U_j. \tag{5}$$

3. Fundamental Algorithm of FT-HPM

The main objective in this section is to develop the homotopy perturbation method using Fourier transform to obtain a new technique. To explain the fundamental algorithm of this technique, we reformulate Eq. (1a) as follows:

$$L(U) + R(U) + N(U) = q(x) \tag{6}$$

with the initial condition $U(x,0)$, where $L = \partial^n / \partial t^n$ is the linear differential operator, R is the linear differential operator of less order than L, N denotes the general nonlinear differential operator, and $q(x)$ represents the source term. Moreover, the main steps of this method can be summarized as follows:

By using the HPM, we have

$$(1-p)[L(U) - L(u_0)] + p[A(U) - q(x)] = 0. \tag{7}$$

Taking the Fourier transform on both sides of Eq. (7), we get

$$\mathcal{F}\big[(1-p)[L(U) - L(u_0)] + p[A(U) - q(x)]\big] = 0, \tag{8}$$

where, $\mathcal{F}[g(t)] = \mathcal{F}(\omega) = \int_{-\infty}^{\infty} g(t) e^{-i\omega t}\, dt$.

Postulate that $A(U) = L(U) + R(U) + N(U)$ and $L = \frac{\partial^n}{\partial t^n}$, then, we obtain

$$\mathcal{F}\left[\frac{\partial^n}{\partial t^n}(U)\right] = \mathcal{F}[L(u_0)] - p\mathcal{F}[L(u_0)] - p\mathcal{F}[R(U) + N(U) - q(x)]. \tag{9}$$

According to the homotopy perturbation method, we assume that

$$U = \sum_{j=0}^{\infty} p^j U_j, \tag{10a}$$

and the non-linear term can be expressed as follows

$$N(U) = \sum_{j=0}^{\infty} p^j H_j. \tag{10b}$$

Where $H_j(U)$ are He's polynomials [47] that are given by:

$$H_j(U_0, U_1, U_2, \ldots, U_j) = \frac{1}{j!}\frac{\partial^j}{\partial p^j}[N(\sum_{i=0}^{\infty} p^i U_i)]_{p=0}, j = 0,1,2,3,\ldots \tag{11}$$

Substituting Eqs. (10a) and (10b) in to Eq. (9), we get

$$\mathcal{F}\left[\frac{\partial^n}{\partial t^n}\sum_{j=0}^{\infty} p^j U_j\right] = \mathcal{F}[L(u_0)] - p\mathcal{F}[L(u_0)] - p\mathcal{F}\left[R\left(\sum_{j=0}^{\infty} p^j U_j\right) + \sum_{m=0}^{\infty} p^j H_j - q(x)\right]. \tag{12}$$

Using the differentiation property of the Fourier transform, we have

$$(i\omega)^n \mathcal{F}\left[\sum_{j=0}^{\infty} p^j U_j\right] = \mathcal{F}[L(u_0)] - p\mathcal{F}[L(u_0)] - p\mathcal{F}\left[R\left(\sum_{j=0}^{\infty} p^j U_j\right) + \sum_{m=0}^{\infty} p^j H_j - q(x)\right]. \tag{13}$$

The rearrangement of Eq. (13), leads to

$$\mathcal{F}\left[\sum_{j=0}^{\infty} p^j U_j\right] = \frac{1}{(i\omega)^n}\mathcal{F}[L(u_0)] - \frac{1}{(i\omega)^n} p\mathcal{F}\left[L(u_0) + R\left(\sum_{j=0}^{\infty} p^j U_j\right) + \sum_{m=0}^{\infty} p^j H_j - q(x)\right]. \tag{14}$$

Now applying the inverse Fourier transform on both sides of Eq. (14), we get

$$\sum_{j=0}^{\infty} p^j U_j = \mathcal{F}^{-1}\left[\frac{1}{(i\omega)^n}\mathcal{F}[L(u_0)]\right] - \mathcal{F}^{-1}\left[\frac{1}{(i\omega)^n} p\mathcal{F}\left[\begin{matrix} L(u_0) + R\left(\sum_{j=0}^{\infty} p^j U_j\right) \\ + \sum_{m=0}^{\infty} p^j H_j - q(x) \end{matrix}\right]\right]. \tag{15}$$

Comparing the coefficient of like powers of p, we have

$$p^0: U_0 = \mathcal{F}^{-1}\left[\frac{1}{(i\omega)^n}\mathcal{F}[L(u_0)]\right],$$

$$p^1: U_1 = -\mathcal{F}^{-1}\left[\frac{1}{(i\omega)^n}\mathcal{F}\left[L(u_0) + R\left(U_0(x)\right) + H_0(U) - q(x)\right]\right],$$

$$p^2: U_2 = -\mathcal{F}^{-1}\left[\frac{1}{(i\omega)^n}\mathcal{F}\left[R\left(U_1(x)\right) + H_1(U)\right]\right],$$

$$\vdots$$

$$p^j: U_j = -\mathcal{F}^{-1}\left[\frac{1}{(i\omega)^n}\mathcal{F}\left[R\left(U_{j-1}(x)\right) + H_{j-1}(U)\right]\right]. \tag{16}$$

Setting $p = 1$, then the analytical approximate solution u is given by

$$u = \lim_{p\to 1} U = \sum_{j=0}^{\infty} U_j. \tag{17}$$

4. Mathematical Formulation

Let us consider the problem of the heat and mass transfer in the unsteady 2D squeezing flow of an incompressible viscous fluid between the infinite parallel plates. Fig. 1 displays the flow geometry and coordinate system. The governing equations for this problem can be described as follows [2]:

$$\frac{\partial U}{\partial x} + \frac{\partial V}{\partial y} = 0, \tag{18a}$$

$$\frac{\partial U}{\partial t} + U\frac{\partial U}{\partial x} + U\frac{\partial U}{\partial y} = -\frac{1}{\rho}\frac{\partial P}{\partial x} + v\left(\frac{\partial^2 U}{\partial x^2} + \frac{\partial^2 U}{\partial y^2}\right), \tag{18b}$$

$$\frac{\partial V}{\partial t} + U\frac{\partial V}{\partial x} + V\frac{\partial V}{\partial y} = -\frac{1}{\rho}\frac{\partial P}{\partial y} + v\left(\frac{\partial^2 V}{\partial x^2} + \frac{\partial^2 V}{\partial y^2}\right), \tag{18c}$$

$$\frac{\partial T}{\partial t} + U\frac{\partial T}{\partial x} + V\frac{\partial T}{\partial y} = \frac{k}{\rho C_P}\left(\frac{\partial^2 T}{\partial x^2} + \frac{\partial^2 T}{\partial y^2}\right) + \frac{v}{C_P}\left(4\left(\frac{\partial U}{\partial x}\right)^2 + \left(\frac{\partial U}{\partial x} + \frac{\partial V}{\partial y}\right)^2\right), \tag{18d}$$

$$\frac{\partial C}{\partial t} + U\frac{\partial C}{\partial x} + V\frac{\partial C}{\partial y} = D\left(\frac{\partial^2 C}{\partial x^2} + \frac{\partial^2 C}{\partial y^2}\right) - K_1(t)C, \tag{18e}$$

With the following boundary conditions

$$U = 0, V = \frac{dh}{dt}, T = T_H, C = C_H \text{ at } y = h(t),$$

$$V = \frac{\partial U}{\partial y} = \frac{\partial T}{\partial y} = \frac{\partial C}{\partial y} = 0, \text{ at } y = 0.$$

Where U, V are the components of velocity in the x- and y-directions respectively, T indicates the temperature, P is the pressure, v is the kinematic viscosity, C is the concentration, ρ is the fluid density, k is the thermal conductivity, D is the coefficient of diffusion of the diffusing species, C_P refers to the specific heat, $h(t) = l\sqrt{1-\alpha t}$ is the distance between two plates, $K_1(t) = \frac{k}{1-\alpha t}$ is the rate of the reaction and α is the squeezing rate, so that the two plates are squeezed until they contact each other when $\alpha > 0$ and $t = \frac{1}{\alpha}$, while the two plates are separated when $\alpha < 0$.

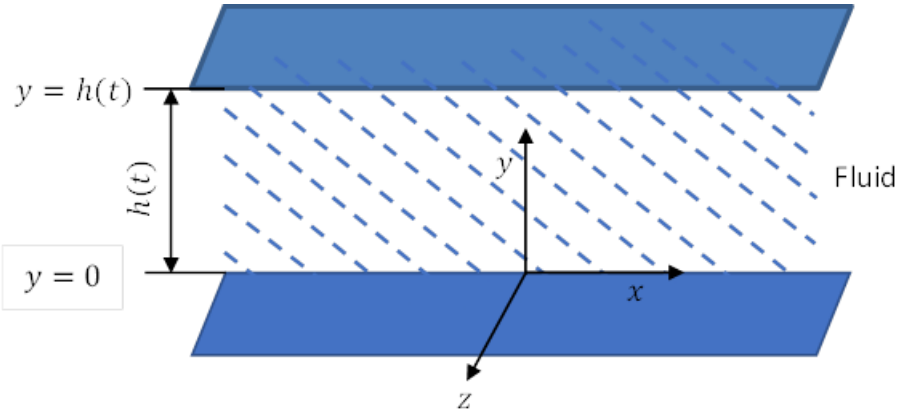

Fig. 1. Schematic diagram of the problem

By using the idea of similarity transformation [2-6]:

$$\eta = \frac{y}{l\sqrt{1-\alpha t}}, U(x,y,t) = \frac{\alpha x}{2(1-\alpha t)}f'(\eta), V(x,y,t) = \frac{\alpha l}{2\sqrt{1-\alpha t}}f(\eta), \theta = \frac{T}{T_H}, \phi = \frac{C}{C_H}. \tag{19}$$

By substituting the variables of Eq. (19) into Eqs. (18b) and (18c), the pressure gradient can be excluded from the resulting equations. Moreover, we will obtain an ordinary differential equation in the following form:

$$f'''' - S(\xi f''' + 3f'' + f'f'' - ff''') = 0. \tag{20}$$

In addition, by using Eq. (19), the Eqs. (18d) and (18e) can be reduced to the following ordinary differential equations

$$\theta'' + PrS(f - \xi)\theta' + PrEc((f'')^2 + 4\delta^2(f')^2) = 0. \tag{21}$$

$$\phi'' + ScS(f - \xi)\phi' - Sc\beta\phi = 0. \tag{22}$$

Subject to the boundary conditions:

$$\left.\begin{aligned} &f(0) = 0\,, f''(0) = 0\,, f(1) = 1\,, f'(1) = 0,\\ &\theta'(0) = 0\,, \theta(1) = 1\,, \phi'(0) = 0\,, \phi(1) = 1, \end{aligned}\right\} \tag{23}$$

where, Pr, S, Sc and Ec refers to the Prandtl number, the squeeze number, the Schmidt number and the Eckert number, respectively, β the parameter of chemical reaction and δ denotes to the Darcy number, all mentioned quantities are defined as follows:

$$S = \frac{\alpha l^2}{2v}\,, Pr = \frac{\mu C_P}{k}\,, Ec = \frac{1}{C_P T_H}\left(\frac{\alpha x}{2(1-\alpha t)}\right)^2, Sc = \frac{v}{D}\,, \beta = \frac{kl^2}{v}\,, \delta = \frac{1}{x}. \tag{24}$$

It is necessary to note that the motion of the plates can be described by the squeeze number S (the case of $S > 0$ corresponds to plates that are moving apart, while the case of $S > 0$ corresponds to the plates that are moving together), in addition, it is noted $\beta > 0$ indicates the destructive chemical reaction and $\beta < 0$ represents the generative chemical reaction.

The physical quantities that will be discussed in this work are the coefficient of skin friction, Nusselt number and Sherwood number which are given as follows [2, 3]:

$$\left.\begin{aligned} C_f &= \frac{\mu\left(\frac{\partial U}{\partial y}\right)_{y=h(t)}}{\rho v_w^2}, \quad \Longrightarrow \frac{l^2}{x^2}(1-\alpha t)ReC_f = -f''(1),\\ Nu &= \frac{-lk\left(\frac{\partial T}{\partial y}\right)_{y=h(t)}}{kT_H}, \quad \Longrightarrow \sqrt{(1-\alpha t)}Nu = -\theta'(1),\\ Sh &= \frac{-lD\left(\frac{\partial C}{\partial y}\right)_{y=h(t)}}{DC_H}, \quad \Longrightarrow \sqrt{(1-\alpha t)}Sh = -\phi'(1). \end{aligned}\right\} \tag{25}$$

5. Application of FT-HPM

In this section, the algorithm of FT-HPM will be used to obtain approximate analytical solutions to the problem of heat and mass transfer with unsteady 2D squeezing viscous flow, moreover, the basic steps of this method can be applied to Eq. (20), Eq. (21) and Eq. (22) with the boundary conditions (23) as follows:

Applying the HPM, we have

$$(1-p)[f'''' - f_0''''] + p[f'''' - S(\xi f''' + 3f'' + f'f'' - ff''')] = 0, \tag{26}$$

$$(1-p)[\theta'' - \theta_0''] + p\begin{bmatrix}\theta'' + PrS(f-\xi)\theta' + \\ PrEc((f'')^2 + 4\delta^2(f')^2)\end{bmatrix} = 0, \tag{27}$$

$$(1-p)[\phi'' - \phi_0''] + p[\phi'' + ScS(f-\xi)\phi' - Sc\beta\phi] = 0. \tag{28}$$

Since, $f_0(\xi) = \theta_0(\xi) = \phi_0(\xi) = 0$, then Eqs. (26), (27) and (28) become

$$f'''' = p[S(\xi f''' + 3f'' + f'f'' - ff''')], \tag{29}$$

$$\theta'' = -p[PrS(f-\xi)\theta' + PrEc((f'')^2 + 4\delta^2(f')^2)], \tag{30}$$

$$\phi'' = -p[ScS(f-\xi)\phi' - Sc\beta\phi]. \tag{31}$$

By taking the Fourier transform on both sides of Eqs. (29), (30) and (31), we get

$$\mathcal{F}[f''''] = p\mathcal{F}[S(\xi f''' + 3f'' + f'f'' - ff''')], \tag{32}$$

$$\mathcal{F}[\theta''] = -p\mathcal{F}[PrS(f\theta' - \xi\theta') + PrEc((f'')^2 + 4\delta^2(f')^2)], \tag{33}$$

$$\mathcal{F}[\phi''] = -p\mathcal{F}[ScS(f\phi' - \xi\phi') - Sc\beta\phi]. \tag{34}$$

According to the assumption of the homotopy perturbation method, we have

$$f = \sum_{j=0}^{\infty} p^j f_j \ , \ \theta = \sum_{j=0}^{\infty} p^j \theta_j \ , \ \phi = \sum_{j=0}^{\infty} p^j \phi_j, \tag{35}$$

Substituting Eq. (35) into Eqs. (32), (33) and (34) we get

$$\mathcal{F}\left[\sum_{j=0}^{\infty} p^j f_j''''\right] = p\mathcal{F}\left[S\begin{pmatrix} \xi \sum_{j=0}^{\infty} p^j f_j''' - \left(\sum_{j=0}^{\infty} p^j f_j\right)\left(\sum_{j=0}^{\infty} p^j f_j'''\right) \\ +3\sum_{j=0}^{\infty} p^j f_j'' + \left(\sum_{j=0}^{\infty} p^j f_j'\right)\left(\sum_{j=0}^{\infty} p^j f_j''\right) \end{pmatrix}\right], \tag{36}$$

$$\mathcal{F}\left[\sum_{j=0}^{\infty} p^j \theta_j''\right] = -p\mathcal{F}\begin{bmatrix} PrS\left(\left(\sum_{j=0}^{\infty} p^j f_j\right)\left(\sum_{j=0}^{\infty} p^j \theta_j'\right) - \xi \sum_{j=0}^{\infty} p^j \theta_j'\right) \\ +PrEc\left(\sum_{j=0}^{\infty} p^j f_j''\right)^2 + 4\delta^2\left(\sum_{j=0}^{\infty} p^j f_j'\right)^2 \end{bmatrix}, \tag{37}$$

$$\mathcal{F}\left[\sum_{j=0}^{\infty} p^j \phi_j''\right] = -p\mathcal{F}\begin{bmatrix} ScS\left(\left(\sum_{j=0}^{\infty} p^j f_j\right)\left(\sum_{j=0}^{\infty} p^j \phi_j'\right) - \xi \sum_{j=0}^{\infty} p^j \phi_j'\right) \\ -Sc\beta \sum_{j=0}^{\infty} p^j \phi_j \end{bmatrix}. \tag{38}$$

Comparing the coefficient of like powers of p, we get

$$p^0: \begin{cases} \mathcal{F}[f_0''''] = 0 & \Rightarrow f_0'''' = 0 \\ \mathcal{F}[\theta_0''] = 0 & \Rightarrow \theta_0'' = 0, \\ \mathcal{F}[\phi_0''] = 0 & \Rightarrow \phi_0'' = 0 \end{cases} \tag{39a}$$

$$\left.\begin{matrix} f_0(0) = 0 \, , f_0''(0) = 0 \, , \ f_0(1) = 1 \, , f_0'(1) = 0, \\ \theta_0'(0) = 0 \, , \theta_0(1) = 1 \, , \phi_0'(0) = 0 \, , \phi_0(1) = 1, \end{matrix}\right\}, \tag{39b}$$

$$p^1: \begin{cases} \mathcal{F}[f_1''''] = \mathcal{F}[S(\xi f_0''' + 3f_0'' + f_0'f_0'' - f_0f_0''')] \\ \mathcal{F}[\theta_1''] = -\mathcal{F}[PrS(f_0\theta_0' - \xi\theta_0') + PrEc(f_0'')^2 + 4\delta^2(f_0')^2], \\ \mathcal{F}[\phi_1''] = -\mathcal{F}[ScS(f_0\phi_0' - \xi\phi_0') - Sc\beta\phi_0] \end{cases} \tag{40a}$$

$$\left.\begin{matrix} f_1(0) = 0 \, , f_1''(0) = 0 \, , \ f_1(1) = 0 \, , f_1'(1) = 0, \\ \theta_1'(0) = 0 \, , \theta_1(1) = 0 \, , \phi_1'(0) = 0 \, , \phi_1(1) = 0, \end{matrix}\right\}, \tag{40b}$$

$$p^2: \begin{cases} \mathcal{F}[f_2''''] = \mathcal{F}[S(\xi f_1''' + 3f_1'' + f_0'f_1'' + f_1'f_0'' - f_0f_1''' - f_1f_0''')] \\ \mathcal{F}[\theta_2''] = -\mathcal{F}[PrS(f_0\theta_1' + f_1\theta_0' - \xi\theta_1') + 2PrEcf_0''f_1'' + 8\delta^2 f_0'f_1'], \\ \mathcal{F}[\phi_2''] = -\mathcal{F}[ScS(f_0\phi_1' + f_1\phi_0' - \xi\phi_1') - Sc\beta\phi_1] \end{cases} \tag{41a}$$

$$\left.\begin{matrix} f_2(0) = 0 \, , f_2''(0) = 0 \, , \ f_2(1) = 0 \, , f_2'(1) = 0, \\ \theta_2'(0) = 0 \, , \theta_2(1) = 0 \, , \phi_2'(0) = 0 \, , \phi_2(1) = 0, \end{matrix}\right\}, \tag{41b}$$

$$p^3: \begin{cases} \mathcal{F}[f_3''''] = \mathcal{F}\left[S\begin{pmatrix} \xi f_2''' + 3f_2'' + f_0'f_2'' + f_1'f_1'' + \\ f_2'f_0'' - f_0f_2''' - f_1f_1''' - f_2f_0''' \end{pmatrix}\right] \\ \mathcal{F}[\theta_3''] = -\mathcal{F}\begin{bmatrix} PrS(f_0\theta_2' + f_1\theta_1' + f_2\theta_0' - \xi\theta_2') + \\ PrEc\{2f_0''f_2'' + (f_1'')^2\} + 4\delta^2\{2f_0'f_2' + (f_1')^2\} \end{bmatrix}, \\ \mathcal{F}[\phi_3''] = -\mathcal{F}[ScS(f_0\phi_2' + f_1\phi_1' + f_2\phi_0' - \xi\phi_2') - Sc\beta\phi_2] \end{cases} \tag{42a}$$

$$\left.\begin{matrix} f_3(0) = 0 \, , f_3''(0) = 0 \, , \ f_3(1) = 0 \, , f_3'(1) = 0, \\ \theta_3'(0) = 0 \, , \theta_3(1) = 0 \, , \phi_3'(0) = 0 \, , \phi_3(1) = 0, \end{matrix}\right\}. \tag{42b}$$

$\vdots$

To solve the system of Eqs. (39a), we use the integration with respect to ξ subject to the boundary conditions in Eq.

(39b), to get

$$f_0(\xi)=\frac{3}{2}\xi-\frac{1}{2}\xi^3\,,\ \theta_0(\xi)=1\,,\ \phi_0(\xi)=1. \tag{43}$$

The systems (40a), (41a) and (42a) represent a non-homogeneous ordinary differential equation. Moreover, its general solutions can be written in the following forms

$$\left.\begin{matrix} f_j(\xi)=f_{j_p}(\xi)+f_{j_c}(\xi) \\ \theta_j(\xi)=\theta_{j_p}(\xi)+\theta_{j_c}(\xi) \\ \phi_j(\xi)=\phi_{j_p}(\xi)+\phi_{j_c}(\xi) \end{matrix}\right\};\ \left.\begin{matrix} f_{j_c}(\xi)=\frac{a_j}{6}\xi^3+\frac{b_j}{2}\xi^2+c_j\xi+d_j \\ \theta_{j_c}(\xi)=p_j\xi+q_j \\ \phi_{j_c}(\xi)=r_j\xi+s_j \end{matrix}\right\},\ j\geq 1, \tag{44}$$

Subject to the boundary conditions

$$\left.\begin{matrix} f_j(0)=0\,,f_j''(0)=0\,,\ f_j(1)=0\,,f_j'(1)=0, \\ \theta_j'(0)=0\,,\theta_j(1)=0\,,\phi_j'(0)=0\,,\phi_j(1)=0. \end{matrix}\right\} \tag{45}$$

The particular solutions $f_{j_p}(\xi)$, $\theta_{j_p}(\xi)$ and $\phi_{j_p}(\xi)$ can be found by applying the fundamental steps of FT-HPM as below:

Using the differentiation property of the Fourier transform on systems (40a), (41a) and (42a) we get

$$\left.\begin{matrix} \mathcal{F}\left[f_{1_p}\right]=\frac{1}{\omega^4}\mathcal{F}[S(\xi f_0'''+3f_0''+f_0'f_0''-f_0f_0''')] \\ \mathcal{F}\left[\theta_{1_p}\right]=\frac{1}{\omega^2}\mathcal{F}[PrS(f_0\theta_0'-\xi\theta_0')+PrEc(f_0'')^2+4\delta^2(f_0')^2] \\ \mathcal{F}\left[\phi_{1_p}\right]=\frac{1}{\omega^2}\mathcal{F}[ScS(f_0\phi_0'-\xi\phi_0')-Sc\beta\phi_0] \end{matrix}\right\}, \tag{46a}$$

$$\left.\begin{matrix} \mathcal{F}\left[f_{2_p}\right]=\frac{1}{\omega^4}\mathcal{F}[S(\xi f_1'''+3f_1''+f_0'f_1''+f_1'f_0''-f_0f_1'''-f_1f_0''')] \\ \mathcal{F}\left[\theta_{2_p}\right]=\frac{1}{\omega^2}\mathcal{F}[PrS(f_0\theta_1'+f_1\theta_0'-\xi\theta_1')+2PrEcf_0''f_1''+8\delta^2f_0'f_1'] \\ \mathcal{F}\left[\phi_{2_p}\right]=\frac{1}{\omega^2}\mathcal{F}[ScS(f_0\phi_1'+f_1\phi_0'-\xi\phi_1')-Sc\beta\phi_1] \end{matrix}\right\}, \tag{46b}$$

$$\left.\begin{matrix} \mathcal{F}\left[f_{3_p}\right]=\frac{1}{\omega^4}\mathcal{F}\left[S\begin{pmatrix}\xi f_2'''+3f_2''+f_0'f_2''+f_1'f_1''+\\ f_2'f_0''-f_0f_2'''-f_1f_1'''-f_2f_0'''\end{pmatrix}\right] \\ \mathcal{F}\left[\theta_{3_p}\right]=\frac{1}{\omega^2}\mathcal{F}\begin{bmatrix}PrS(f_0\theta_2'+f_1\theta_1'+f_2\theta_0'-\xi\theta_2')+\\ PrEc\{2f_0''f_2''+(f_1'')^2\}+4\delta^2\{2f_0'f_2'+(f_1')^2\}\end{bmatrix} \\ \mathcal{F}\left[\phi_{3_p}\right]=\frac{1}{\omega^2}\mathcal{F}[ScS(f_0\phi_2'+f_1\phi_1'+f_2\phi_0'-\xi\phi_2')-Sc\beta\phi_2] \end{matrix}\right\}. \tag{46c}$$

$\vdots$

The inverse Fourier transform on both sides of systems. (46a), (46b) and (46c) gives

$$\left.\begin{matrix} f_{1_p}=\mathcal{F}^{-1}\left(\frac{1}{\omega^4}\mathcal{F}[S(\xi f_0'''+3f_0''+f_0'f_0''-f_0f_0''')]\right) \\ \theta_{1_p}=\mathcal{F}^{-1}\left(\frac{1}{\omega^2}\mathcal{F}[PrS(f_0\theta_0'-\xi\theta_0')+PrEc(f_0'')^2+4\delta^2(f_0')^2]\right) \\ \phi_{1_p}=\mathcal{F}^{-1}\left(\frac{1}{\omega^2}\mathcal{F}[ScS(f_0\phi_0'-\xi\phi_0')-Sc\beta\phi_0]\right) \end{matrix}\right\}, \tag{47a}$$

$$\left.\begin{matrix} f_{2_p}=\mathcal{F}^{-1}\left(\frac{1}{\omega^4}\mathcal{F}[S(\xi f_1'''+3f_1''+f_0'f_1''+f_1'f_0''-f_0f_1'''-f_1f_0''')]\right) \\ \theta_{2_p}=\mathcal{F}^{-1}\left(\frac{1}{\omega^2}\mathcal{F}[PrS(f_0\theta_1'+f_1\theta_0'-\xi\theta_1')+2PrEcf_0''f_1''+8\delta^2f_0'f_1']\right) \\ \phi_{2_p}=\mathcal{F}^{-1}\left(\frac{1}{\omega^2}\mathcal{F}[ScS(f_0\phi_1'+f_1\phi_0'-\xi\phi_1')-Sc\beta\phi_1]\right) \end{matrix}\right\}, \tag{47b}$$

$$\left.\begin{aligned} f_{3_p} &= \mathcal{F}^{-1}\left(\frac{1}{\omega^4}\mathcal{F}\left[S\begin{pmatrix}\xi f_2''' + 3f_2'' + f_0' f_2'' + f_1' f_1'' + \\ f_2' f_0'' - f_0 f_2''' - f_1 f_1''' - f_2 f_0'''\end{pmatrix}\right]\right) \\ \theta_{3_p} &= \mathcal{F}^{-1}\left(\frac{1}{\omega^2}\mathcal{F}\left[\begin{matrix}PrS(f_0\theta_2' + f_1\theta_1' + f_2\theta_0' - \xi\theta_2') + \\ PrEc\{2f_0'' f_2'' + (f_1'')^2\} + 4\delta^2\{2f_0' f_2' + (f_1')^2\}\end{matrix}\right]\right) \\ \phi_{3_p} &= \mathcal{F}^{-1}\left(\frac{1}{\omega^2}\mathcal{F}[ScS(f_0\phi_2' + f_1\phi_1' + f_2\phi_0' - \xi\phi_2') - Sc\beta\phi_2]\right) \end{aligned}\right\}. \quad (47c)$$

$\vdots$

The simplification of system (44) leads to the following solutions

$$f_1(\xi) = \frac{1}{280}S(\xi^7 + 28\xi^5 + 83\xi^3 - 26\xi), \quad (48)$$

$$\theta_1(\xi) = -\frac{3\delta^2}{20}PrEc[2\xi^6 - 10\xi^4 + 30\xi^2 - 22] - \frac{3}{20}PrEc[5\xi^4 - 5], \quad (49)$$

$$\phi_1(\xi) = \frac{1}{2}Sc\beta[\xi^2 - 1], \quad (50)$$

$$f_2(\xi) = \frac{1}{3880800}S^2\begin{bmatrix}42\xi^{11} + 1925\xi^9 - 38214\xi^7 + 149616\xi^5 - \\ 187100\xi^3 - 76431\xi\end{bmatrix}, \quad (51)$$

$$\theta_2(\xi) = -\frac{1}{8400}PrSEc\begin{bmatrix}(84Pr\delta^2 - 28\delta^2)\xi^{10} - \begin{pmatrix}585Pr\delta^2 - 945\delta^2 \\ -225Pr + 135\end{pmatrix}\xi^8 \\ +(2100Pr\delta^2 - 3588\delta^2 - 420Pr + 3360)\xi^6 - \\ (3150Pr\delta^2 - 5550\delta^2 + 4770)\xi^4 - 4680\delta^2\xi^2 \\ 1551Pr\delta^2 + 1801\delta^2 + 195Pr + 1545\end{bmatrix}, \quad (52)$$

$$\phi_2(\xi) = \frac{1}{120}Sc^2\beta[2S\xi^6 - (5S + 5\beta)\xi^4 - 30\beta\xi^2 + 3S + 25\beta], \quad (53)$$

$$f_3(\xi) = \frac{1}{7063056000}S^3\begin{bmatrix}931\xi^{15} + 12740\xi^{13} + 148876\xi^{11} - 3923920\xi^9 \\ +24455743\xi^7 - 68104400\xi^5 + 7770991\xi^3 - \\ 30299884\xi\end{bmatrix}, \quad (54)$$

$$\theta_3(\xi) = \begin{bmatrix}\frac{-1}{3640}\left(Pr^3Ec\delta^2S^2 - \frac{97}{210}Pr^2Ec\delta^2S^2 + \frac{3}{140}PrEc\delta^2S^2\right)\xi^{14} + \\ \frac{PrEc\delta^2}{504504000}\begin{pmatrix}286650Pr - 255346Pr\delta^2 \\ -409500Pr^2 + 581490\delta^2 \\ +1255800Pr^2\delta^2 - 58695\end{pmatrix}\xi^{12} + \cdots\end{bmatrix}, \quad (55)$$

$$\phi_3(\xi) = \frac{1}{15200}Sc^2\beta\begin{bmatrix}(14S^2Sc - S^2)\xi^{10} - (60S^2Sc - 45SSc - 45S^2)\xi^8 \\ +(70S^2Sc - 315SSc\beta + 35\beta^2 - 159S^2)\xi^6 + \cdots\end{bmatrix}. \quad (56)$$

$\vdots$

The approximate analytical solutions f, θ and ϕ are given by truncated series

$$f = \lim_{N\to\infty}\sum_{j=0}^{N} f_j\ ,\ \theta = \lim_{N\to\infty}\sum_{j=0}^{N}\theta_j\ ,\ \phi = \lim_{N\to\infty}\sum_{j=0}^{N}\phi_j. \quad (57)$$

6. Results and Discussion

In this section, the influence of physical parameters on velocity, temperature, concentration, coefficient of skin friction, Nusselt number and Sherwood number will be discussed.

Fig. 2 illustrates the effects of positive and negative values of squeeze number on $f(\xi)$ and $f'(\xi)$. It can be seen that, the velocity $f(\xi)$ increases whilst $f'(\xi)$ decreasing from $\xi = 0$ to $\xi = 1$. It's clear that, when the squeeze number increases, the amount of velocity will decrease slightly, while the velocity reaches its highest value at the lowest value of S, while $f'(\xi)$ changes its effect with the value of S as $\xi > 0.4$.

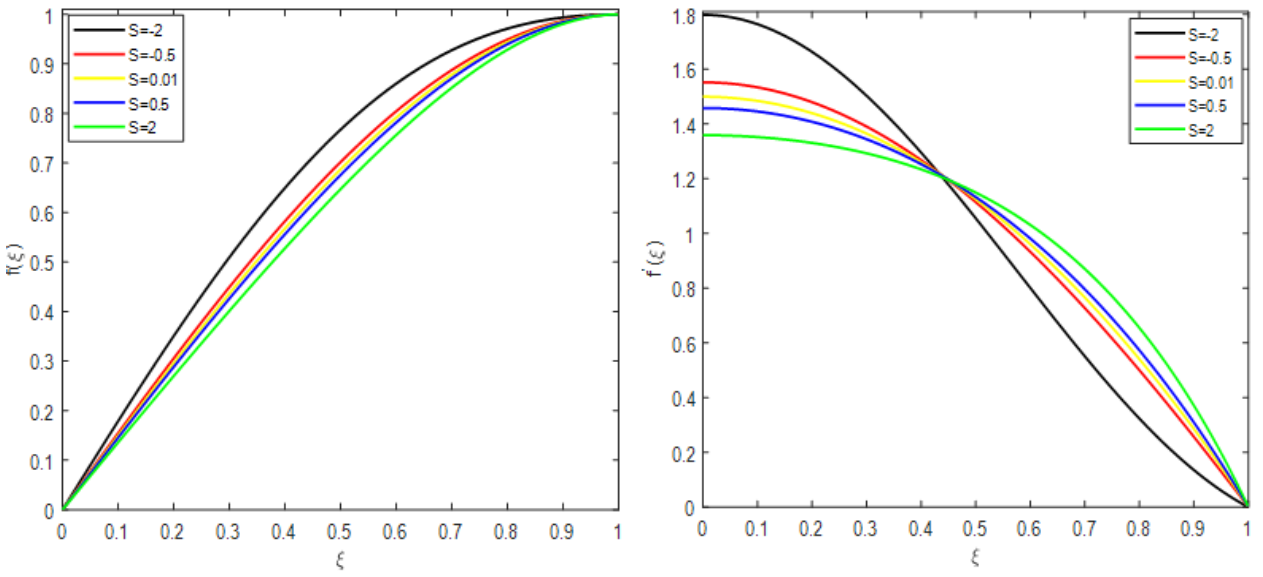

Fig. 2. Influence of squeeze number S on $f(\xi)$ and $f'(\xi)$

The influence of the squeeze number S, Prandtl number Pr and Eckert number Ec on the temperature $\theta(\xi)$ are explained in Fig. 3a, Fig. 3b and Fig. 3c, respectively. It is noted that an increase in the S values leads to a decrease in the temperature values, because any increase in the value of S is associated with the increase of the distance between the plates, the increase in the plate motion and a decrease in the viscosity of kinematic. Liquid materials with high thermal diffusivity and low viscosity are characterized by having Pr values less than one, while high viscosity materials are characterized by Pr values greater than one, moreover, we notice that the increase in the Pr values leads to an increase in the values of temperature. The Eckert number Ec is used to describe the relationship between the thickness of thermal boundary layer and the kinetic energy of the flow. So, it has been observed that an increase in the values of Ec leads to an increase in the amount of $\theta(\xi)$.

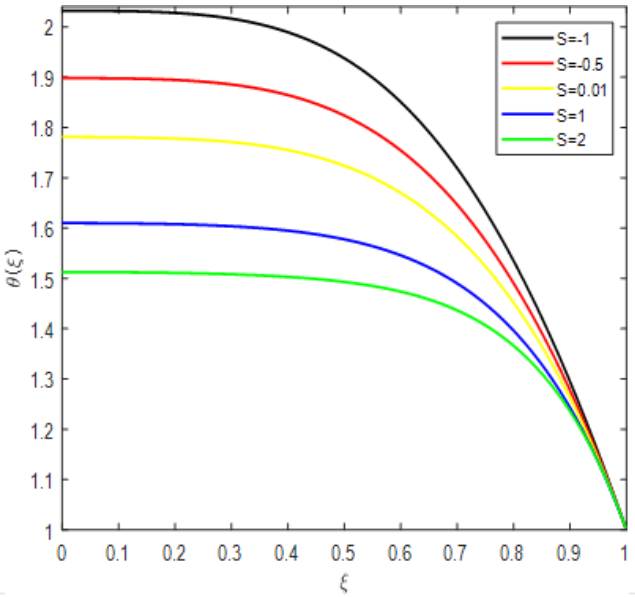

Fig. 3a. Influence of S on $\theta(\xi)$ at $Pr = Ec = 1$ and $\delta = 0.1$

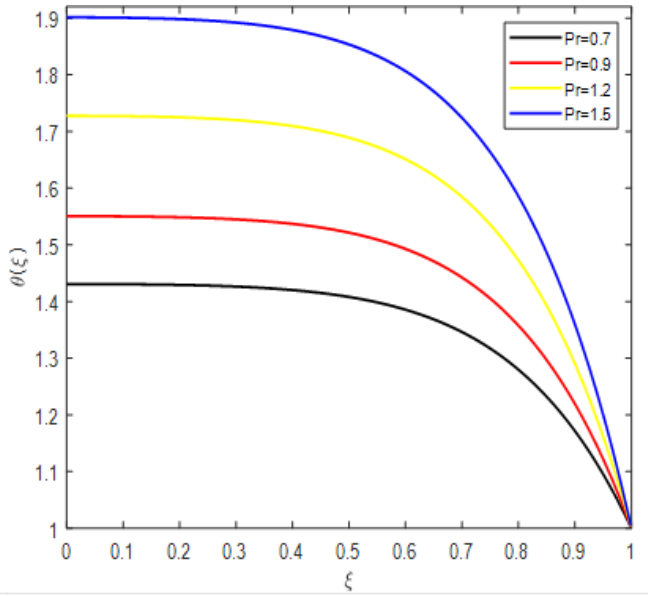

Fig. 3b. Influence of Pr on $\theta(\xi)$ at $S = Ec = 1$ and $\delta = 0.1$

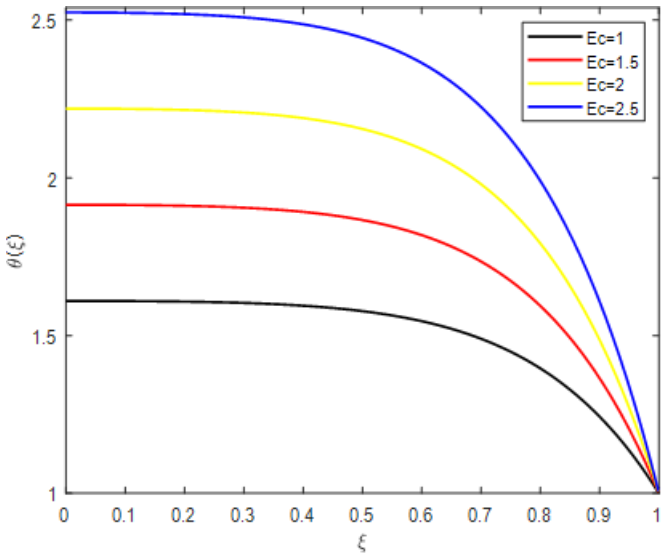

Fig. 3c. Influence of Ec on $\theta(\xi)$ at $Pr = S = 1$ and $\delta = 0.1$

In Figs. (4a, 4b and 4c) show the effect of squeeze, Schmidt and chemical reaction numbers on the concentration, respectively. In Fig. 4a, we observe that the increase in the values of S leads to an increase in $\phi(\xi)$. While it is noted in Fig. 4b that the increase in Sc values, which represents the ratio between molecular diffusion and kinematic viscosity, leads to a decrease in molecular diffusion. In addition, it has been observed that the values of $\phi(\xi)$ are inversely proportional to the chemical reaction as shown in Fig. 4c.

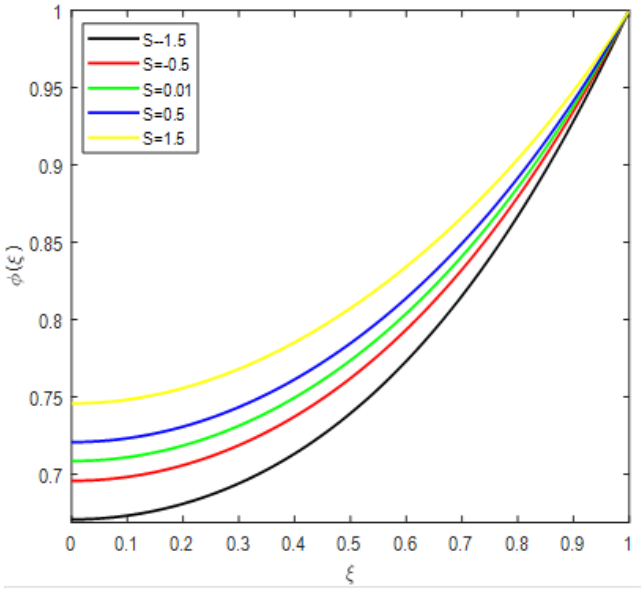

Fig. 4a. Influence of S on $\phi(\xi)$. at $Sc = \beta = 1$

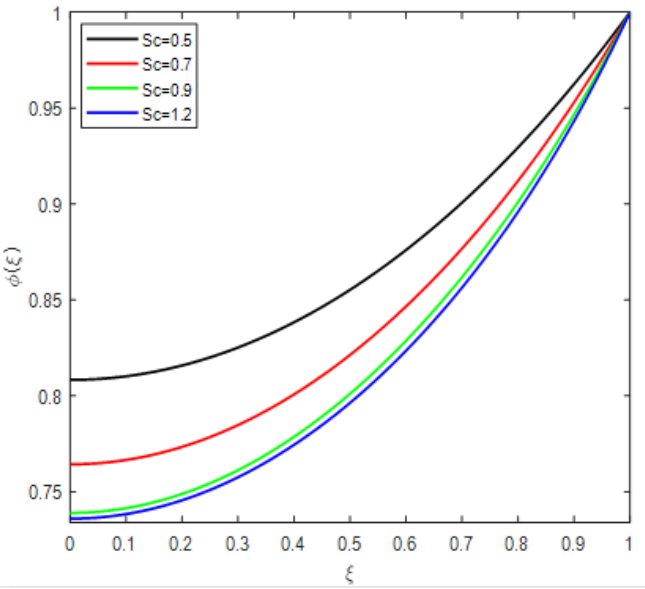

Fig. 4b. Influence of Sc on $\phi(\xi)$. at $S = \beta = 1$

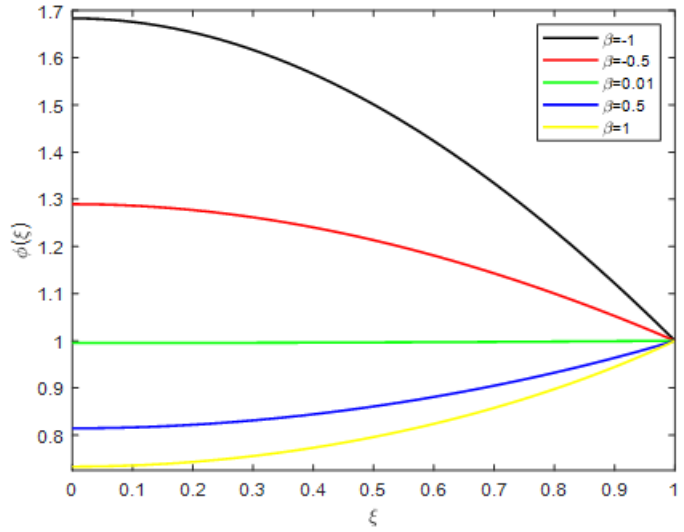

Fig. 4c. Influence of β on $\phi(\xi)$. at $Sc = S = 1$

Table (1-a, b) presenting the comparison of the computed values of $f(\xi)$, $\theta(\xi)$ and $\phi(\xi)$ between FT-HPM and PIA [10] atThe values . $Sc$and Pr, $S$with different values of the active parameters $\beta = 1$and $\delta = 0.1$, $Ec = 0.5$ calculated by the approved method (FT-HPM) for skin friction coefficient and Nusselt number were compared with the values calculated by HAM [2], CWM [48] and WGM [12] at various values of S with $Pr = Ec = 1$ and $\delta = 0.1$, and as shown in Table (2-a, b). Table (3) and Table (4) illustrate the comparison values of Nusselt number $-\theta'(1)$ and the local Sherwood number $\phi'(1)$ between FT-HPM and the previous results in PIA [10], HAM [2], ADM [3] and CM and LSM in [5] for various values of Pr and Ec at $S = 0.5$ and $\delta = 0.1$, respectively. Through the tables that were mentioned, we notice a good agreement between the results of the current work and the previously published results.

Table 1a: The comparison of computed values of $f(\xi)$, $\theta(\xi)$ and $\phi(\xi)$ between FT-HPM and PIA [10] at $Ec = 0.5, \delta = 0.1, \beta = 1, S = 1, Pr = 0.7$ and $Sc = 1$.

ξ	$f(\xi)$		$\theta(\xi)$		$\phi(\xi)$	
	FT-HPM	PIA [10]	FT-HPM	PIA [10]	FT-HPM	PIA [10]
0	0	0	1.227896	1.223609	0.794002	0.793084
0.1	0.141906	0.141911	1.227738	1.223454	0.796024	0.795097
0.2	0.281703	0.281713	1.227086	1.222826	0.802089	0.801141
0.3	0.417195	0.417210	1.225388	1.221222	0.812207	0.811232
0.4	0.546012	0.546029	1.221671	1.217726	0.826392	0.825398
0.5	0.665517	0.665535	1.214443	1.210878	0.844670	0.843682
0.6	0.772715	0.772731	1.199150	1.198474	0.867082	0.866146
0.7	0.864147	0.864159	1.179625	1.177244	0.893693	0.892874
0.8	0.935783	0.935790	1.144047	1.142370	0.924603	0.923981
0.9	0.982910	0.982912	1.087688	1.086768	0.959963	0.959622
1	1	1	1	1	1	1

Table 1b: The comparison of computed values of $f(\xi)$, $\theta(\xi)$ and $\phi(\xi)$ between FT-HPM and PIA [10]at $Ec = 0.5, \delta = 0.1, \beta = 1, S = 0.5, Pr = 2$ and $Sc = 0.5$.

ξ	$f(\xi)$		$\theta(\xi)$		$\phi(\xi)$	
	FT-HPM	PIA [10]	FT-HPM	PIA [10]	FT-HPM	PIA [10]
0	0	0	1.687521	1.685384	0.623769	0.625275
0.1	0.145379	0.145379	1.687044	1.684908	0.627375	0.628926
0.2	0.288250	0.288250	1.684990	1.682864	0.638206	0.639883
0.3	0.426053	0.426054	1.679454	1.677366	0.656309	0.658161
0.4	0.556129	0.556130	1.667128	1.665131	0.681763	0.683790
0.5	0.675668	0.675670	1.643087	1.641254	0.714689	0.716828
0.6	0.781659	0.781660	1.599441	1.598853	0.755254	0.757379
0.7	0.870838	0.870838	1.529813	1.528542	0.803690	0.805613
0.8	0.939636	0.939636	1.418565	1.417662	0.860312	0.861806
0.9	0.984132	0.984132	1.249658	1.249170	0.925552	0.926383
1	1	1	1	1	1	1

Table 2a: Comparison the coefficient of skin friction $-f''(1)$ by FT-HPM with the results in [2, 10-12] at various values of S for $Pr = Ec = 1$ and $\delta = 0.1$

S	$-f''(1)$				
	FT-HPM	PIA [10]	HAM [2]	CWM [48]	WGM [49]
-1	2.175727	2.175046	2.170090	2.170090	2.170090
-0.5	2.617708	2.617667	2.614038	2.617403	2.617403
0.01	3.007133	3.007133	3.007134	3.007133	3.007133
0.5	3.336688	3.336652	3.336449	3.336449	3.336449
2	4.213994	4.205992	4.167389	4.167389	4.167389

Table 2b: The comparison of computed values of Nusselt number $-\theta'(1)$ by FT-HPM with the results in [2, 10-12] at various values of S for $Pr = Ec = 1$ and $\delta = 0.1$

S	$-\theta'(1)$				
	FT-HPM	PIA [10]	HAM [2]	CWM [48]	WGM [49]
-1	3.255970	3.296785	3.319899	3.319899	3.319899
-0.5	3.122983	3.127831	3.129491	3.129491	3.129491
0.01	3.047091	3.047091	3.047092	3.047091	3.048091
0.5	3.031021	3.026661	3.026324	3.026323	3.026323
2	3.096093	3.092889	3.118551	3.026323	3.118549

Table 3: Comparison the values of Nusselt number $-\theta'(1)$ between FT-HPM and the results in [2, 3, 5, 6] for various values of Pr and Ec at $S = 0.5$ and $\delta = 0.1$.

Pr	Ec	FT-HPM	PIA [10]	HAM [2]	ADM [3]	LSM [5]	CM [5]
0.5	1	1.524288	1.522364	1.522368	1.522367	1.520649	1.526577
1		3.031021	3.026661	3.026324	3.026323	3.023438	3.03732
2		5.993945	5.982991	5.980530	5.980530	5.976762	6.012625
5		14.51669	14.46871	14.43941	14.43941	14.44158	14.59172
1	0.5	1.515510	1.513330	1.513162	1.513161	1.511719	1.518660
	1.2	3.637225	3.631993	3.631588	3.631588	3.628125	3.644784
	2	6.062042	6.053323	6.052647	6.052647	6.046876	6.074640
	5	15.15510	15.13330	15.13162	15.13161	15.11719	15.18660

Table 4: Comparison between FT-HPM, PIA [10] and HAM [2] of local Sherwood number $\phi'(1)$ for different values of Sc and β when $S = 0.5$ and $\delta = 0.1$

Sc	β	FT-HPM	PIA [10]	HAM [2]	Sc	β	FT-HPM	PIA [10]	HAM [2]
0.5	1	0.428511	0.428301	0.424826	1	-0.5	-0.578650	-0.578851	-0.581206
1		0.793015	0.791485	0.744224		-0.1	-0.100149	-0.100138	-0.100139
1.5		1.211964	1.206977	0.990645		0.5	0.423888	0.423445	0.419225
2		1.803809	1.792201	1.211277		1	0.793015	0.791485	0.744224

Now: To study the efficiency and accuracy of the proposed method (FT-HPM), the error norms L_1, L_2 and L_∞ that resulted from finding approximate analytical solutions to the current problem were calculated. Tables (5-a,b), showing the comparison of computed errors of $f(\xi)$, $\theta(\xi)$ and $\phi(\xi)$ with CPU time between FT-HPM and PIA [10] at $Ec = 0.5, \delta = 0.1, \beta = 1$ with various values of S, Pr and Sc.

Table 5.a: The comparison of computed errors of $f(\xi)$, $\theta(\xi)$ and $\phi(\xi)$ between FT-HPM and PIA [10] at $Ec = 0.5, \delta = 0.1, \beta = 1, S = 1, Pr = 0.7$ and $Sc = 1$.

	$f(\xi)$		$\theta(\xi)$		$\phi(\xi)$	
Error	FT-HPM	PIA [10]	FT-HPM	PIA [10]	FT-HPM	PIA [10]
L_1	3.00×10^{-7}	5.95×10^{-4}	2.47×10^{-5}	7.16×10^{-3}	6.14×10^{-5}	6.86×10^{-2}
L_2	5.48×10^{-4}	6.97×10^{-4}	4.97×10^{-3}	8.09×10^{-3}	7.83×10^{-3}	7.56×10^{-2}
L_∞	5.60×10^{-4}	1.06×10^{-3}	5.32×10^{-3}	1.06×10^{-2}	1.49×10^{-2}	1.04×10^{-1}
CPUs	0.015	0.031	0.016	0.291	0.016	0.063

Table 5.b: The comparison of computed errors of $f(\xi)$, $\theta(\xi)$ and $\phi(\xi)$ between FT-HPM and PIA [10] at $Ec = 0.5, \delta = 0.1, \beta = 1, S = 0.5, Pr = 2$ and $Sc = 0.5$.

	$f(\xi)$		$\theta(\xi)$		$\phi(\xi)$	
Error	FT-HPM	PIA [10]	FT-HPM	PIA [10]	FT-HPM	PIA [10]
L_1	2.30×10^{-9}	7.50×10^{-5}	3.69×10^{-5}	8.81×10^{-3}	4.89×10^{-7}	7.73×10^{-3}
L_2	4.79×10^{-5}	8.78×10^{-5}	6.08×10^{-3}	9.67×10^{-3}	7.00×10^{-4}	8.54×10^{-3}
L_∞	4.85×10^{-5}	1.33×10^{-4}	6.56×10^{-3}	1.23×10^{-2}	144×10^{-3}	1.19×10^{-2}
CPUs	0.016	0.063	0.031	0.296	0.016	0.063

It is clear from the above tables that the error norms using FT-HPM are lower than the error norms using PIA. In addition, we notice that the computational time of the norm errors resulting from FT-HPM is less than the computational time of the norm errors generated by PIA, moreover, we find that the new method (FT-HPM) has higher accuracy and efficiency than PIA.

7. Convergence Analysis of FT-HPM

In this section, we will provide some important definitions for the study of convergence analysis with finding the necessary condition for the convergence of the approximate analytical solutions of the FT-HPM technique for the problem of heat and mass transfer with unsteady 2D squeezing viscous flow.

Definition 7.1: Let $\mathcal{M}: \mathcal{H} \longrightarrow \mathbb{R}$ be a non-linear mapping, where $\mathcal{H}$, $\mathbb{R}$ represents the Banach space, the set of real numbers, respectively. Then, the sequence of the solutions can be given as

$$E_{n+1} = \mathcal{M}(E_n),\ E_n = \sum_{j=0}^{n} h_j,\ j = 0,1,2,3,\ldots \tag{58}$$

where, $\mathcal{M}$ fulfills the Lipschitz condition which is given by the following formula:

$$\|\mathcal{M}(E_n) - \mathcal{M}(E_{n-1})\| \le \gamma \|E_n - E_{n-1}\|,\ 0 < \gamma < 1. \tag{59}$$

Theorem 2.1: The necessary condition for the convergence of the solutions series $h = \sum_{j=0}^{\infty} h_j$ that is obtained by the based algorithms, is achieving of the following property:

$$\|E_{n+1} - E_n\| \to 0 \text{ as } n \to \infty \text{ for } 0 < \gamma < 1. \tag{60}$$

Proof:

$$\begin{aligned}
\|E_{n+1} - E_n\| &= \left\|\sum_{j=0}^{n+1} h_j - \sum_{j=0}^{n} h_j\right\| = \left\| h_0 + \sum_{j=1}^{n+1} h_j - \left[h_0 + \sum_{j=1}^{n} h_j\right] \right\| \\
&= \left\| h_0 + \sum_{j=1}^{n+1} L_1^{-1}[W_{j-1}] - \left\{h_0 + \sum_{j=1}^{n} L_1^{-1}[W_{j-1}]\right\} \right\| \\
&= \left\| h_0 + L_1^{-1}\sum_{j=1}^{n+1}[W_{j-1}] - \left\{h_0 + L_1^{-1}\sum_{j=1}^{n}[W_{j-1}]\right\} \right\|
\end{aligned}$$

Since, $E_{n+1} = \mathcal{M}(E_n)$, then

$$\begin{aligned}
\|E_{n+1} - E_n\| &= \left\|L_1^{-1}\mathcal{M}\sum_{j=0}^{n}[W_{j-1}] - L_1^{-1}\mathcal{M}\sum_{j=0}^{n-1}[W_{j-1}]\right\| \\
&= \left\| L_1^{-1}\mathcal{M}\left[\sum_{j=0}^{n} h_j\right] - L_1^{-1}\mathcal{M}\left[\sum_{j=0}^{n-1} h_j\right] \right\| \\
&\le |L_1^{-1}| \left\| \mathcal{M}\left[\sum_{j=0}^{n} h_j\right] - \mathcal{M}\left[\sum_{j=0}^{n-1} h_j\right] \right\| \\
&\le \gamma \left\| \sum_{j=0}^{n} L_1^{-1}[W_{j-1}] - \sum_{j=0}^{n-1} L_1^{-1}[W_{j-1}] \right\| \\
&\le \gamma^2 \left\|\sum_{j=0}^{n-1} L_1^{-1}[W_{j-1}] - \sum_{j=0}^{n-2} L_1^{-1}[W_{j-1}]\right\| \\
&\ \vdots \\
&\le \gamma^n \left\|\sum_{j=0}^{1} L_1^{-1}[W_{j-1}] - \sum_{j=0}^{0} L_1^{-1}[W_{j-1}]\right\| \\
&= \gamma^n \|E_1 - E_0\| \to 0 \text{ as } n \to \infty \text{ for } 0 < \gamma < 1.
\end{aligned}$$

■

The results of the above theorem, can be used to find the powers of the parameter γ by formulating the following definition.

Definition 7.2 For $n = 1,2,3,\ldots$

$$\gamma^n = \begin{cases} \dfrac{\|E_{n+1} - E_n\|}{\|E_1 - E_0\|} = \dfrac{\|h_{n+1}\|}{\|h_1\|}, \|h_1\| \ne 0, n = 1,2,3,\ldots \\ 0, \qquad\qquad \|h_1\| = 0 \end{cases} \tag{61}$$

Eq. (61) can be used to find the convergence of approximate solutions to the current problem. Moreover, the results of convergence of solutions that were found were compared using the two methods FT-HPM, HPM, as shown in the following tables:

Table 6a: Comparison of the computed values of γ^n for $f(\xi)$, $\theta(\xi)$ and $\phi(\xi)$ between FT-HPM and HPM at $Ec = 0.5, \delta = 0.1, \beta = 1, S = 1, Pr = 0.7$ and $Sc = 1$.

	$f(\xi)$		$\theta(\xi)$		$\phi(\xi)$	
γ^n	FT-HPM	HPM	FT-HPM	HPM	FT-HPM	HPM
γ^1	0.15×10^{-1}	1.92×10^{-1}	0.75×10^{-1}	2.39×10^{-1}	0.12×10^{-2}	4.60×10^{-1}
γ^2	0.91×10^{-4}	0.41×10^{-1}	0.42×10^{-2}	0.83×10^{-1}	0.22×10^{-4}	2.20×10^{-1}
⋮	⋮	⋮	⋮	⋮	⋮	⋮

Table 6b: Comparison of the computed values of γ^n for $f(\xi)$, $\theta(\xi)$ and $\phi(\xi)$ between FT-HPM and HPM at $Ec = 0.5, \delta = 0.1, \beta = 1, S = 0.5, Pr = 2$ and $Sc = 0.5$.

	$f(\xi)$		$\theta(\xi)$		$\phi(\xi)$	
γ^n	FT-HPM	HPM	FT-HPM	HPM	FT-HPM	HPM
γ^1	0.75×10^{-2}	0.96×10^{-1}	0.29×10^{-1}	1.40×10^{-1}	0.42×10^{-2}	2.16×10^{-1}
γ^2	0.22×10^{-4}	0.10×10^{-1}	0.92×10^{-3}	0.26×10^{-1}	0.51×10^{-5}	0.47×10^{-1}
⋮	⋮	⋮	⋮	⋮	⋮	⋮

It is clear from tables (6-a, b) that $\gamma^n \to 0$ as $n \to \infty$ for $0 < \gamma < 1$. In addition, this tables show that the powers of γ which were calculated based on FT-HPM approach to zero faster than the powers of γ calculated by HPM. Therefore, FT-HPM can be considered as a development of HPM with better convergence.

8. Conclusions

In this paper, FT-HPM was applied to find analytical approximate solutions to the problem of heat and mass transfer of the unsteady 2D squeezing flow of an incompressible viscous fluid between infinite parallel plates, and when discussing the effect of physical parameters on the resulting solutions, we obtained the following conclusions:

• The tabular and graphical results showed the possibility of using the new technique (FT-HPM), and they are consistent with the results of previously published studies [2, 5, 10, 11].

• From Table (5-a, b) the error norms using FT-HPM are lower than the error norms using PIA. In addition, we notice that the computational time of the norm errors resulting from FT-HPM is less than the computational time of the norm errors generated by PIA, moreover, we find that the new method (FT-HPM) has higher accuracy and efficiency than PIA.

• When comparing the algorithm of the new technique (FT-HPM) with the algorithm of HPM, as shown in Table (6-a, b), we notice that FT-HPM has better convergence than HPM, which indicates that the new method FT-HPM represents a development of the HPM method.

• From the tables and graphs of the velocity f, we notice that the positive and negative values of the squeeze number S have an inverse effect on the velocity.

• The temperature field increases with increasing the values of Pr and Ec, while the temperature field decreases with increasing the squeeze number S.

• The magnitude of the local Nusselt number can be represented by an increasing function of Pr and Ec.

• The concentration profile values decrease when the Schmidt number Sc increases, while the magnitude of the local Sherwood number increases with the increase of *Sc*

• The field of Concentration ϕ represents decreasing function of the parameter of destructive chemical reaction ($\beta > 0$), while it represents an increasing function of the parameter of generative chemical reaction ($\beta < 0$).

• An increase in the value of β leads to an increase in the magnitude of the local Sherwood number.

References:

[1] M. Mahmood, S. Asghar, M. Hossain, Squeezed flow and heat transfer over a porous surface for viscous fluid, *Heat and mass Transfer*, Vol. 44, pp. 165-173, 2007.

[2] M. Mustafa, T. Hayat, S. Obaidat, On heat and mass transfer in the unsteady squeezing flow between parallel plates, *Meccanica*, Vol. 47, pp. 1581-1589, 2012.

[3] M. Sheikholeslami, D. Ganji, H. Ashorynejad, Investigation of squeezing unsteady nanofluid flow using ADM, *Powder Technology*, Vol. 239, pp. 259-265, 2013.

[4] M. Sheikholeslami, M. Hatami, G. Domairry, Numerical simulation of two phase unsteady nanofluid flow and heat transfer between parallel plates in presence of time dependent magnetic field, *Journal of the Taiwan Institute of Chemical Engineers*, Vol. 46, pp. 43-50, 2015.

[5] O. Pourmehran, M. Rahimi-Gorji, M. Gorji-Bandpy, D. Ganji, RETRACTED: analytical investigation of squeezing unsteady nanofluid flow between parallel plates by LSM and CM, Elsevier, 2015.

[6] K. Singh, S. K. Rawat, M. Kumar, Heat and mass transfer on squeezing unsteady MHD nanofluid flow between parallel plates with slip velocity effect, *Journal of Nanoscience*, Vol. 2016, 2016.

[7] G. M. Sobamowo, A. Akinshilo, Double diffusive magnetohydrodynamic squeezing flow of nanofluid between two parallel disks with slip and temperature jump boundary conditions, *Applied and Computational Mechanics*, Vol. 11, No. 2, 2017.

[8] N. Balazadeh, M. Sheikholeslami, D. D. Ganji, Z. Li, Semi analytical analysis for transient Eyring-Powell squeezing flow in a stretching channel due to magnetic field using DTM, *Journal of Molecular Liquids*, Vol. 260, pp. 30-36, 2018.

[9] M. Atlas, S. Hussain, M. Sagheer, Entropy generation and unsteady Casson fluid flow squeezing between two parallel plates subject to Cattaneo-Christov heat and mass flux, *The European Physical Journal Plus*, Vol. 134, No. 1, pp. 33, 2019.

[10] A.-S. Al-Saif, A. Harfash, Perturbation-iteration algorithm for solving heat and mass transfer in the unsteady squeezing flow between parallel plates, *Journal of Applied and Computational Mechanics*, Vol. 5, No. 4, pp. 804-815, 2019.

[11] A. Gupta, S. S. Ray, Numerical treatment for investigation of squeezing unsteady nanofluid flow between two parallel plates, *Powder Technology*, Vol. 279, pp. 282-289, 2015.

[12] S. H. Seyedi, B. N. Saray, A. Ramazani, On the multiscale simulation of squeezing nanofluid flow by a highprecision scheme, *Powder Technology*, Vol. 340, pp. 264-273, 2018.

[13] J.-H. He, A coupling method of a homotopy technique and a perturbation technique for non-linear problems, *International Journal of Non-Linear Mechanics*, Vol. 35, No. 1, pp. 37-43, 2000/01/01/, 2000.

[14] J.-H. He, The homotopy perturbation method for nonlinear oscillators with discontinuities, *Applied mathematics and computation*, Vol. 151, No. 1, pp. 287-292, 2004.

[15] J.-H. He, Homotopy perturbation technique, *Computer methods in applied mechanics and engineering*, Vol. 178, No. 3-4, pp. 257-262, 1999.